



HAL
open science

NC α - gem -dimethylated peptoid side chains: A novel approach for structural control and peptide sequence mimetics

Radhe Shyam, Lionel Nauton, Gaetano Angelici, Olivier Roy, Claude Taillefumier, Sophie Faure

► To cite this version:

Radhe Shyam, Lionel Nauton, Gaetano Angelici, Olivier Roy, Claude Taillefumier, et al.. NC α -gem -dimethylated peptoid side chains: A novel approach for structural control and peptide sequence mimetics. *Biopolymers*, 2019, 110, pp.e23273. 10.1002/bip.23273 . hal-02194898

HAL Id: hal-02194898

<https://hal.science/hal-02194898>

Submitted on 13 Oct 2021

HAL is a multi-disciplinary open access archive for the deposit and dissemination of scientific research documents, whether they are published or not. The documents may come from teaching and research institutions in France or abroad, or from public or private research centers.

L'archive ouverte pluridisciplinaire **HAL**, est destinée au dépôt et à la diffusion de documents scientifiques de niveau recherche, publiés ou non, émanant des établissements d'enseignement et de recherche français ou étrangers, des laboratoires publics ou privés.

***N*C α -*gem*-dimethylated peptoid side chains: a novel approach for structural control and peptide sequence mimetics.**

Radhe Shyam, Lionel Nauton, Gaetano Angelici, Olivier Roy, Claude Taillefumier, Sophie Faure

Université Clermont Auvergne, CNRS, SIGMA Clermont, ICCF, F-63000 Clermont-Ferrand, France

sophie.faure@uca.fr

ABSTRACT

The design of linear peptoid oligomers adopting well-defined secondary structures while mimicking defined peptide primary sequences is a major challenge in the context of drug discovery. To this end, chemists have developed *cis*-inducing peptoid side chains to build robust PolyProline I-type helices. However, the number of efficient examples remains scarce and chemical diversity accessible through the use of these side chains remains limited. Herein, we introduce an array of *N*C α -*gem*-dimethylated peptoid residues mimicking proteinogenic amino acids. Submonomer synthesis and block-coupling approaches were explored to access heterooligomers incorporating these novel types of side chains. NMR studies of monomer and trimer models showed that the *N*C α -*gem*-dimethylated groups exert a complete *cis* control on the backbone amide conformation. Lastly, a preliminary molecular modelling study gave an insight into the preferred orientation of the substituents of the *N*C α -*gem*-dimethyl side chains relative to the peptoid backbone.

1 INTRODUCTION

Ever since their initial development in 1992,¹ *N*-substituted glycine oligomers or “peptoids”, have been considered a highly promising class of protease resistant peptidomimetics due to their close similarity to peptides. Peptoids are sequence-defined oligomers that are generally synthesized by the robust “submonomer method” wherein each peptoid residue is created in two steps: an acylation step to create the peptoid carbon backbone followed by a substitution step using primary amines to install the side chains.² This methodology is particularly well-suited for the preparation of large combinatorial peptoid libraries.³ Although chemically similar to peptides, peptoids do not retain their folding properties, primarily due to the absence of backbone intramolecular hydrogen bonding capacity and an achiral backbone. Furthermore, the *cis/trans* isomerism of the main chain *N,N*-disubstituted amides also contributes to the conformational heterogeneity of the peptoid backbone. This may hamper the development of peptoid ligands with high and selective affinity for biological targets, including the development of folded peptoids as blockers of relevant protein-protein interactions. It is therefore essential to develop strategies for the control of peptoid folding while retaining the unique chemical diversity. Peptoid chemists have developed specific side chains capable of controlling the amide conformation by forming local interactions with the backbone. This has enabled the design of peptoid oligomers exhibiting various privileged secondary structures such as helices (Polyproline type I (PPI),⁴ Polyproline type II (PPII)⁵ and η -helix⁶), ribbons,⁷ loops⁸ and Σ -strands.⁹ Despite a modest *cis*-directing control on the tertiary amide bond isomerism, the chiral aromatic phenylethyl side chain (spe) has been used extensively to promote the PPI peptoid helical conformation. Furthermore, its use as helix inducer imposes constraints in term of physicochemical diversity that are a serious brake on the SAR studies.¹⁰ Other strong *cis*-inducing peptoid side chains include the chiral aromatic naphthylethyl (s1npe),¹¹ the triazolium-type side chain,¹² the chiral aliphatic *tert*-butylethyl (s1tbe),¹³ and the achiral aliphatic *tert*-butyl (*t*Bu)¹⁴ and fluoro-alkyl groups.¹⁵

In order to increase chemical diversity, functionalized chiral phenylethyl side chains carrying different substituents on the aromatic core have been developed.¹⁶ However, neither these highly hydrophobic side chains nor the triazolium-type side chains represent optimal mimetics of amino acid side chains.¹⁷ Among the *cis*-inducing peptoid side chains, the *tert*-butyl side chain is unique since it induces complete *cis* conformation *via* steric effects, regardless of the nature of the solvent (Figure 1A).^{14,18} In addition, despite the absence of chirality, a network of weak interactions such as intramolecular CO(*i*)...HC(*i*-*n*) (*n*=1,2 or 3) hydrogen bonds and *i*/*i*+3 *t*Bu...*t*Bu London interactions help the folding of *Nt*Bu peptoid oligomers into the PPI-like helical conformation (Figure 1B).¹⁹

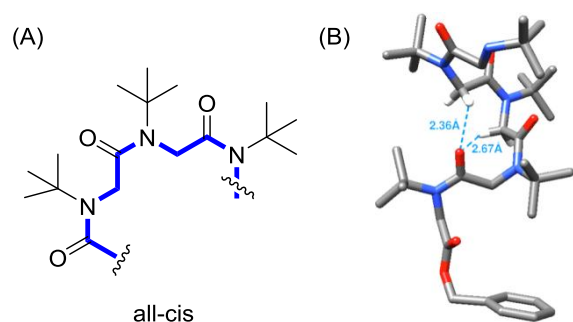


FIGURE 1 (a) Peptoid oligomer carrying the *tert*-butyl side chain; (b) X-Ray structure of the pentamer Ac-(*Nt*Bu)₅-OBn¹⁹

Through the design of *N*C α -*gem*-dimethylated *N*-substituted glycine monomers mimicking natural amino acids (Figure 2), we herein address the challenge of controlling the amide bond isomerism while retaining the chemical diversity. These novel side chains may be regarded as “functionalized” *tert*-butyl side chains and we therefore speculated that they would likewise induce a high or even complete *cis*-amide control.

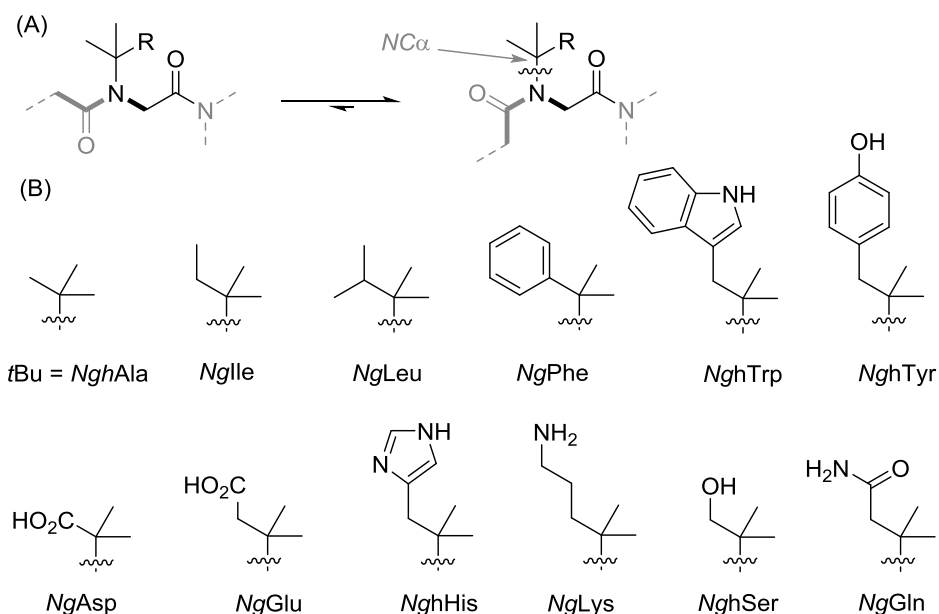


FIGURE 2 (a) Generic structure of a peptoid residue carrying a “substituted” *tert*-butyl side chain and its *cis/trans* isomerism; (b) Structures of a library of α,α -*gem*-dimethylated side chains mimicking proteinogenic amino acids side chains and proposed peptoid residue nomenclature (the *g* letter refers to α,α -*gem*-dimethyl and the *h* letter refers to homo)

The *gem*-dimethyl moiety is a special feature encountered in many natural products such as taxanes, epothilones or macrolides.²⁰ Furthermore, the *gem*-dimethyl group has been successfully introduced in biologically relevant compounds in order to enhance specific therapeutic effects (bioavailability,

potency, selectivity, toxicity). In the field of peptides and peptidomimetics, the Thorpe-Ingold effect of the *gem*-dimethyl group has been exploited for the conformational restriction of peptide oligomers through the use of α -aminoisobutyric acid (Aib).²¹ As mentioned above, we speculated that the steric restriction generated by the *N*C α -*gem*-dimethyl group should block the peptoid backbone amide in the *cis* conformation. Herein we thus show that a large array of *cis* inducing side chains closely mimicking natural amino acids side chains could be designed and introduced into peptoid oligomers.

2 MATERIALS AND METHODS

2.1 Materials

Chemicals obtained from commercial sources were used without further purification unless stated otherwise. *tert*-Butylamine (98% purity), *tert*-amylamine (98% purity), 2-amino-2-methyl-1-propanol (99% purity) and diphenylphosphinic acid pentafluorophenyl ester were purchased from Aldrich. Benzyl bromoacetate (97% purity), ethyl bromoacetate (98% purity) and bromo acetyl bromide (98% purity) were purchased from Alfa aesar. *tert*-Butylbromoacetate (98% purity) was purchased from TCI. Piperidine (99% purity) was purchased from Avocado. THF, CH₂Cl₂ and MeOH were dried over aluminum oxide via a solvent purification system and stored over 4Å molecular sieves. EtOAc, CH₂Cl₂, cyclohexane, and MeOH for column chromatography were obtained from commercial sources and were used as received. Et₃N was dried over KOH, distilled and stored over 4Å molecular sieves.

2.2 Preparation of α,α -*gem*-dimethylated amines

The required *N*C α -*gem*-dimethylated amines **a-g** (Figure 3) were purchased or prepared in gram scale (Supporting Information Scheme S1, S2 and S3).

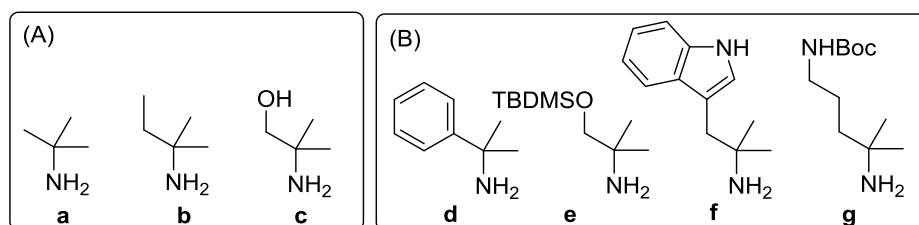


FIGURE 3 List of the α,α -*gem*-dimethylated amines used in the present study: (A) commercially available and (B) amines prepared by synthesis

2.3 Preparation of peptoid monomer models carrying *N*C α -*gem*-dimethylated side chains

To a solution of piperidine (1.0 equiv, 0.2 M) in THF at 0 °C under argon was added Et₃N (1.2 equiv) and then bromoacetyl bromide (1.2 equiv). After stirring for 1 h at 0°C, the resulting mixture was diluted with EtOAc (10 mL per mmol of starting material) and filtered, washing the solids with EtOAc. The filtrate was then concentrated and dried *in vacuo*, yielding *N*-(2-bromo-1-oxoethyl)piperidine which was purified by flash chromatography on silica gel using EtOAc/cyclohexane 50:50 as eluent. To a solution of the bromoacetyl amide (1.0 equiv, 0.2 M) in THF at 0 °C under argon was added Et₃N (2.0 equiv) followed by the chosen α,α -*gem*-dimethylated amine (4.0 equiv). After stirring overnight at room temperature, the resulting mixture was diluted with EtOAc (10 mL per mmol starting material) and filtered, washing the solids with EtOAc. The filtrate was then concentrated under reduced pressure. When the primary amine used could not be removed by simple evaporation, the product was purified by flash chromatography on silica gel. The secondary amine was then acetylated with acetic anhydride (4.0 equiv) and Et₃N (2.0 equiv) in EtOAc at 0 °C

overnight. The resulting mixture was diluted with EtOAc (10 mL per mmol starting material) and filtered, washing the solids with EtOAc. The filtrate was then concentrated and dried *in vacuo*, and the crude monomeric peptoid model was purified by flash chromatography on silica gel.

2.4 Submonomer synthesis of peptoid oligomers

2.4.1 Substitution step

To a solution of *tert*-butyl bromoacetate, benzyl bromoacetate, ethyl bromoacetate or bromoacetyl amide (1.0 equiv, 0.2 M) in THF at 0 °C under argon was added Et₃N (2.0 equiv) followed by the chosen primary amine (4.0 equiv). After stirring overnight at room temperature, the resulting mixture was diluted with EtOAc (10 mL per mmol starting material) and filtered, washing the solids with EtOAc. The filtrate was then concentrated under reduced pressure. EtOAc was added to the residue which was then concentrated under reduced pressure. When the primary amine used could not be removed by simple evaporation under reduced pressure, the product was purified by flash chromatography on silica gel.

2.4.2 Acylation step

To a solution of the crude secondary amine (1.0 equiv, 0.2 M) in EtOAc at 0°C under argon, was added Et₃N (1.2 equiv) and then a solution of freshly prepared bromoacetic anhydride (1.2 equiv) in EtOAc. After stirring for 2 h at room temperature the resulting mixture was filtered, washing the solids with EtOAc. The filtrate was then concentrated and dried *in vacuo*. Flash chromatography on silica gel yielded the desired bromoacetyl amide.

2.4.3 *N*-terminal acetylation

To a solution of the peptoid (1.0 equiv) and Et₃N (4.0 equiv) in EtOAc (0.2 M) at room temperature was added acetic anhydride (8.0 equiv). After stirring overnight at room temperature, the mixture was filtered, washing the solids with EtOAc. The filtrate was then concentrated and dried *in vacuo*, yielding the crude *N*-acylated compound. The final oligomer was purified by flash chromatography on silica gel.

2.5 Access to peptoid oligomers by blockwise coupling approach

2.5.1 General procedure of coupling with pentafluorophenyl diphenyl phosphinate (FDPP)

The required free-acid block peptoid oligomer was obtained by hydrogenolysis of the benzyl ester precursor using Pd/C 10% in methanol. To a solution of the free-acid block peptoid oligomer (1.0 equiv., 0.4M) in dry CH₂Cl₂ at room temperature under argon was added FDPP (1.2 equiv). The mixture was stirred for 5 min and a solution of the free-amine block peptoid oligomer (1.0 equiv., 0.4M) and DBU (3.0 equiv.) in CH₂Cl₂ was slowly added dropwise. The resulting mixture was stirred at room temperature for 48h and was then diluted with CH₂Cl₂ and subsequently washed with 5% aq. citric acid solution and satd. aq. NaHCO₃. The organic fraction was dried over Na₂SO₄, filtered and concentrated *in vacuo*, yielding the crude product. The products were purified by flash chromatography on silica gel column.

2.5.2 General procedure of coupling with pentafluorophenyl trifluoroacetate (TFAPfp)

The required free-acid block peptoid oligomer was obtained by hydrogenolysis of the benzyl ester precursor using Pd/C 10% in methanol. To a solution of the free-acid block peptoid oligomer (1.0

equiv., 0.3M) in dry CH_2Cl_2 at room temperature under argon was added pentafluorophenyl trifluoroacetate (1.5 equiv.) and pyridine (1.5 equiv.). The mixture was stirred for 1 h and was then diluted with CH_2Cl_2 and washed with 1M HCl and satd. aq. NaHCO_3 . The organic fraction was dried over Na_2SO_4 , filtered and concentrated *in vacuo*, yielding the crude activated ester which was immediately used in the next step. To the solution of the activated ester (1.0 equiv., 0.2 M) in dry CH_2Cl_2 at room temperature under argon was added slowly a solution of the free-amine block peptoid oligomer (1.0 equiv., 0.2M) and DBU (3.0 equiv.) in CH_2Cl_2 . The mixture was stirred for 48h and was then diluted with CH_2Cl_2 and subsequently washed with 5% aq. citric acid solution and satd. aq. NaHCO_3 . The organic fraction was dried over Na_2SO_4 , filtered and concentrated *in vacuo*, yielding the crude product. The products were purified by flash chromatography on silica gel column.

2.6 Mass spectrometry

LC-MS were recorded on a Micromass Q-ToF Micro (3000 V) apparatus or a Q Exactive Quadrupole-Orbitrap Mass Spectrometer coupled to a UPLC Ultimate 3000 (Kinetex EVO C18; 1.7 μm ; 100mm x 2.1mm column with a flow rate of 0.45 $\text{mL}\cdot\text{min}^{-1}$ with a linear gradient of solvent B from 5% to 95% over 7.5 min (solvent A = H_2O + 0.1% formic acid, solvent B = acetonitrile + 0.1% formic acid); equipped with a DAD UV/VIS 3000 RS detector).

2.7 Nuclear magnetic resonance spectroscopy

NMR spectra (^1H , ^{13}C , Jmod, COSY, HSQC, HMBC) were recorded on a Bruker AC 400 spectrometer or a Bruker AC-500 spectrometer. Chemical shifts were referenced to the residual solvent peak and coupling values J were given in Hz. The following multiplicity abbreviations were used: s for singlet, bs for broad singlet, d for doublet, t for triplet, q for quartet and m for multiplet. Assignments were based on the following 1D and 2D experiments: ^1H , COSY, HMBC, HSQC and J-mod-experiments.

2.8 Molecular modelling

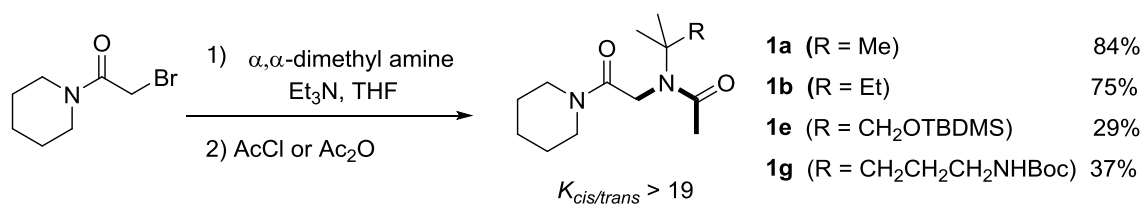
Gas-phase full geometry optimizations and scans were performed at the density functional theory (DFT) level using B3LYP functional with 6-31+G(d,p) basis sets. All the DFT calculations were carried out with Gaussian09 software.²² Structure preparations and visualizations were performed using chimera software.²³

On peptoid monomer models, a 360° scan of the dihedral angle χ_1 was performed by intervals of 5° at the B3LYP/6-31+G(d,p) level. Molecular dynamics was performed using NAMD²⁴ and the charmm22²⁵ force field parameters. A hexamer model was constructed after parametrization of each side chain with Gaussian 09 and using the paratool module from VMD (visual Molecular Dynamic).²⁶ For the initial construction, the ω dihedral angles were considered to be 0° (*cis* conformation), the ϕ dihedral angles were considered to be -90° and the ψ dihedral angles were considered to be $\pm 180^\circ$. The χ_1 angle values were chosen to correspond one of the most stable positions identified during the χ_1 scan of monomer models; for the *tert*-butyl side chain ($\chi_1 = +60^\circ$), for the *Ng*Ile side chain ($\chi_1 = -60^\circ$) and for the *Ng*Phe side chain ($\chi_1 = \pm 180^\circ$). The hexamer was capped with an *N*-terminal acetyl group and a *C*-terminal benzyl ester. The molecular dynamics (MD) simulation included an initial phase of minimization followed by 40 ns of simulation. MD simulation was performed in gas with a dielectric constant of 37.5 corresponding to acetonitrile as solvent, at a temperature of 298K.

3 RESULTS AND DISCUSSION

A large number of α,α -*gem*-dimethyl primary amines are commercially available, including those that are necessary for mimicking the side chain of naturally-occurring amino acids (Figure 2). In the present study, six different $NC\alpha$ -*gem*-dimethyl side chains were installed and their capacity to control the backbone amide conformation was studied. These six side chains originated from the use of *tert*-butylamine **a**, 1,1-dimethylpropylamine **b**, 2-amino-2-methyl-1-propanol **c**, α,α -dimethylbenzylamine **d**, α,α -dimethyl-1*H*-indole-3-ethanamine **f** and *tert*-butyl *N*-(4-amino-4-methylpentyl) carbamate **g** (Figure 3). Although commercially available, amines **d**, **f** and **g** were prepared on gram-scale according to known procedures (Supporting Information).

We first synthesized a series of peptoid monomer models carrying these novel side chains in order to study their capacity to control the peptoid amide geometry. The *cis*-directing effect of these new side chains was thus assessed using a *C*-piperidiny amide monomer model capped with an acetyl group at the *N*-terminus (Scheme 4). This peptoid model has previously proven to be well suited for the determination of amide *cis/trans* ratios.¹¹⁻¹⁵ The *cis/trans* ratio of the acetamide may indeed be investigated by NMR spectroscopy since the *cis* and *trans* rotamers display distinct ¹H NMR resonances which allows for determining $K_{cis/trans}$ ratios.^{11,12} Starting from *N*-(2-bromo-1-oxoethyl) piperidine, bromine substitution with an excess of primary amine in the presence of triethylamine followed by acetylation provided the monomeric models carrying a selection of “functionalized” *tert*-butyl side chains in moderate to good yields (Scheme 1).

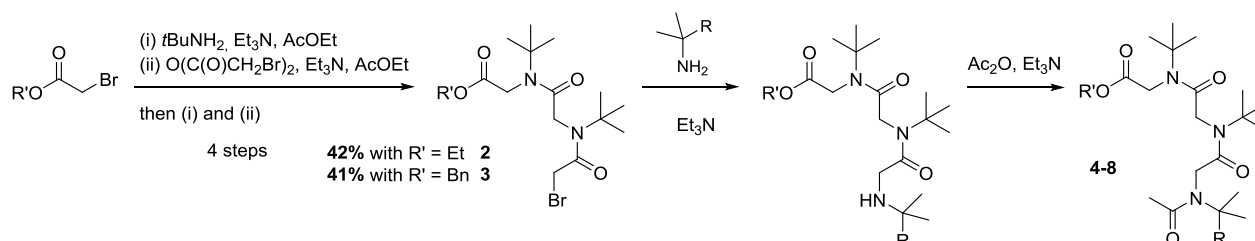


SCHEME 1 Synthesis of peptoid monomer models **1**

As previously described, the steric effect of the *tert*-butyl group results in the presence of only one amide rotamer in the ¹H NMR spectra of monomer **1a** in a variety of solvents (CDCl₃, CD₃CN, CD₃OD, acetone-*d*₆, and D₂O, Supporting Information). This conformation was shown to be *cis* by NOESY experiments.¹⁴ The absence of the *trans* rotamer signals was therefore interpreted as the *tert*-butyl group resulting in a *cis/trans* ratio of > 95:5 ($K_{cis/trans}$ ratio > 19). Importantly, the ¹H NMR spectra of the new peptoid models **1b**, **1e** and **1g** likewise only showed a single set of signals, corresponding to the *cis* conformation of the acetamide ($K_{cis/trans}$ ratio > 19).

The *cis* inducing effect of the $NC\alpha$ -*gem*-dimethyl side chains was further studied on trimeric peptoids. A series of trimers with two consecutive *tert*-butyl side chains and a $NC\alpha$ -*gem*-dimethyl side chain on the terminal acetamide was therefore designed. The trimer models **4-8** (Scheme 2) were prepared following the submonomer solution-phase synthesis methodology using a bromoacetic anhydride-based protocol developed for sterically hindered and deactivated primary amines.¹⁴ When using these optimized conditions and when employing volatile primary amines, chromatography is only required after the acylation step.²⁷ Indeed, only filtration of salts and evaporation are needed after the substitution step. However, when a non-volatile primary amine is used in the substitution reaction, purification by flash chromatography is also required after this step. The use of solid-phase synthesis was avoided since it is our experience that oligomers of different lengths that are difficult to separate are obtained when synthesizing homooligomeric peptoids with *t*Bu side chains. The common bromo intermediates **2** and **3** were prepared in four steps starting from ethyl bromoacetate or benzyl bromoacetate with yields of 42% and 41%, respectively (Scheme 2). Nucleophilic substitution using

the α,α -*gem*-dimethyl amines **c**, **d**, **f** or **g** followed by acetylation provided trimers **4-8** (Table 1). Displacement of the bromide was also achieved with the non-*gem*-dimethylated amine **h** (*N*-Boc-1,4-diaminobutane) to provide peptoid **9** for comparative studies.



SCHEME 2 Synthesis of peptoid trimers **4-8** (conditions (i) for the substitution step and (ii) for the acylation step)

Peptoid trimers	Amines	Yield ^a	Exact mass HRMS (TOF MS ES+)
Ac- <i>Ng</i> Phe- <i>Ngh</i> Ala- <i>Ngh</i> Ala-OEt 4	a , a , d	54%	C ₂₇ H ₄₄ N ₅ O ₃ [M+H ⁺]: calc. 490.3270, found 490.3275
Ac- <i>Ngh</i> Ser- <i>Ngh</i> Ala- <i>Ngh</i> Ala-OBn 5	a , a , c	72%	C ₂₇ H ₄₄ N ₃ O ₆ [M+H ⁺]: calc. 506.3214, found 506.3224
Ac- <i>Ngh</i> Trp- <i>Ngh</i> Ala- <i>Ngh</i> Ala-OBn 6	a , a , f	74%	C ₃₅ H ₄₉ N ₄ O ₅ [M+H ⁺]: calc. 605.3703, found 605.3703
Ac- <i>Ng</i> Lys(Boc)- <i>Ngh</i> Ala- <i>Ngh</i> Ala-OEt 7	a , a , g	28%	C ₂₉ H ₅₅ N ₄ O ₇ [M+H ⁺]: calc. 571.4065, found 571.4053
Ac- <i>Ng</i> Lys(Boc)- <i>Ngh</i> Ala- <i>Ngh</i> Ala-OBn 8	a , a , g	54%	C ₃₄ H ₅₇ N ₄ O ₇ [M+H ⁺]: calc. 633.4227, found 633.4224
Ac- <i>N</i> Lys(Boc)- <i>Ngh</i> Ala- <i>Ngh</i> Ala-OBn 9	a , a , h ^b	57%	C ₃₂ H ₅₃ N ₄ O ₇ [M+H ⁺]: calc. 605.3909, found 605.3892

^aOverall yields calculated from the bromo derivatives **2** or **3**; ^bThe primary amine **h** is *N*-Boc-1,4-diaminobutane.

TABLE 1 Peptoid sequences and yields of trimers **4-9**

The *cis/trans* ratio of the terminal acetamide was determined for all the trimer peptoids **4-9** by ¹H NMR integration of singlets corresponding to the acetyl CH₃ protons (Figure 4). According to previous studies,^{19,28} the protons of *trans* peptoid acetamides are deshielded which results in a chemical shift of > 2 ppm. On the contrary, it was observed that the protons of *cis* acetamides display a chemical shift of < 2 ppm. The ¹H NMR spectrum of trimer **9** in CD₃OD showed two singlets at 1.93 and 2.15 ppm in 48:52 proportion, indicating the presence of two conformational isomers in a 48:52 *cis/trans* ratio. By contrast, the ¹H NMR spectrum in CD₃OD of the corresponding trimer **8** with a *N*C α -*gem*-dimethylated-functionalized lysine side chain showed a major singlet at 1.91 ppm indicating a strong preference for the *cis* conformation of the terminal acetamide. A very small singlet detected at 2.15 ppm may correspond to the *trans* rotamer (< 3%). The same trend was observed for trimers **4**, **5**, **6**, and **7** carrying the *N*C α -*gem*-dimethylated-functionalized phenylalanine, *homo*-serine, *homo*-tryptophan and lysine side chains respectively (Figure 4).

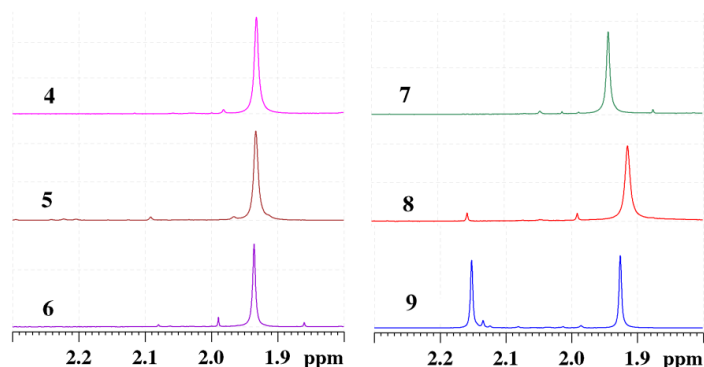
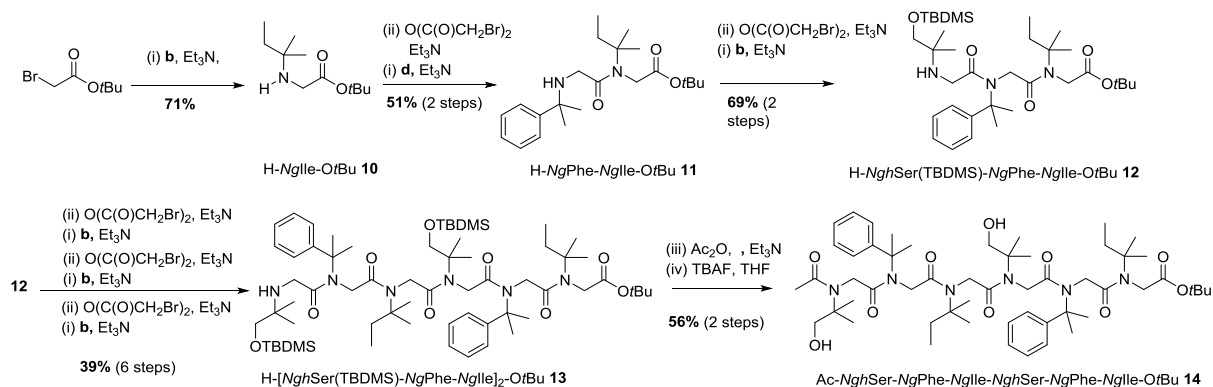


FIGURE 4 Acetyl proton region of the ¹H NMR spectra of trimers **4**, **5**, **6** (on the left) and **7**, **8**, **9** (on the right) in CD₃OD

This NMR study on model trimers clearly indicates that the *N*C α -*gem*-dimethylated side chains have the same highly selective *cis*-directing effect as the *tert*-butyl side chain. This novel family of side chains thus locks the backbone amides in the *cis* conformation while maintaining access to a high

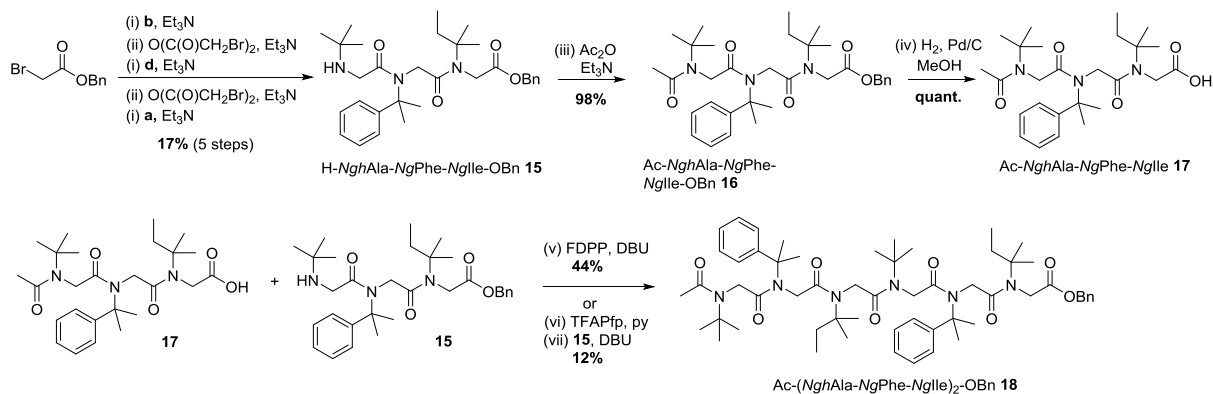
degree of diversity. To further demonstrate the value of *N*C α -*gem*-dimethylated side chains in a drug discovery context we therefore synthesized longer oligomers.

Access to longer oligomers was first explored using the submonomer method. This method was thus used to synthesize peptoid hexamer **14** carrying three different types of *N*C α -*gem*-dimethylated residues: NgPhe, NgIle and NghSer (Scheme 3). The monomer **10** was first synthesized from *tert*-butyl bromoacetate and amine **b**. Five submonomer cycles then furnished the hexamer **13** in a non-optimized overall yield of 10%. Subsequent acetylation using acetic anhydride and *tert*-butyldimethylsilyl deprotection with tetrabutylammonium fluoride furnished the hexapeptoid Ac-(NghSer-NgPhe-NgIle)₂-OtBu **14** as a white powder.



SCHEME 3 Submonomer synthesis of peptoid hexamer Ac-(NghSer-NgPhe-NgIle)₂-OtBu **14** (conditions (i) for the substitution step and (ii) for the acylation step; all oligomers present amide bonds in a dominant *cis* conformation, but are drawn *trans* for convenience)

A convergent fragment-coupling approach which is more appropriate to access longer oligomers was then explored. Using this method, hexamer **18** was synthesized (Scheme 4). First, the trimer block amine **15** and trimer block acid **17** were prepared by submonomer synthesis, incorporating successively the amines **b** (*tert*-amylamine), **d** (α,α -dimethylbenzylamine) and **a** (*tert*-butylamine). The coupling of these two trimers using FDPP as coupling reagent in the presence of 1,8-diazabicyclo[5.4.0]undec-7-ene (DBU) as base, yielded the hexamer **18** in 44% yield. The use of a two-step procedure involving the corresponding activated pentafluorophenyl ester intermediate¹⁹ instead proved less efficient. Indeed, only 12 % of hexamer **18** was formed and nearly 50% of the trimer block amine **15** was recovered after purification of the crude product.



SCHEME 4 Fragment-coupling approach to access peptoid hexamer Ac-(NghAla-NgPhe-NgIle)₂-OBn **18** (conditions (i) for the substitution step and (ii) for the acylation step; all oligomers present amide bonds in a dominant *cis* conformation, but are drawn *trans* for convenience)

In order to provide insight into the preferred orientation of the substituents of the $NC\alpha$ -*gem*-dimethyl side chains with respect to the peptoid backbone, the total energy of peptoid models with the acetamide in the *cis* conformation was determined by a systematic variation of the χ_1 torsion angle by intervals of 5° at the B3LYP/6-31+G(d,p) level (Figure 5). The calculations were performed on *C*-methyl ester peptoid monomers capped with an acetyl group at the *N*-terminus with different $NC\alpha$ -*gem*-dimethyl side chains (models Ac-*Nt*Bu-OMe, Ac-*Ng*Ile-OMe and Ac-*Ng*Phe-OMe) or the isopropyl group (model Ac-*Ni*Pr-OMe).

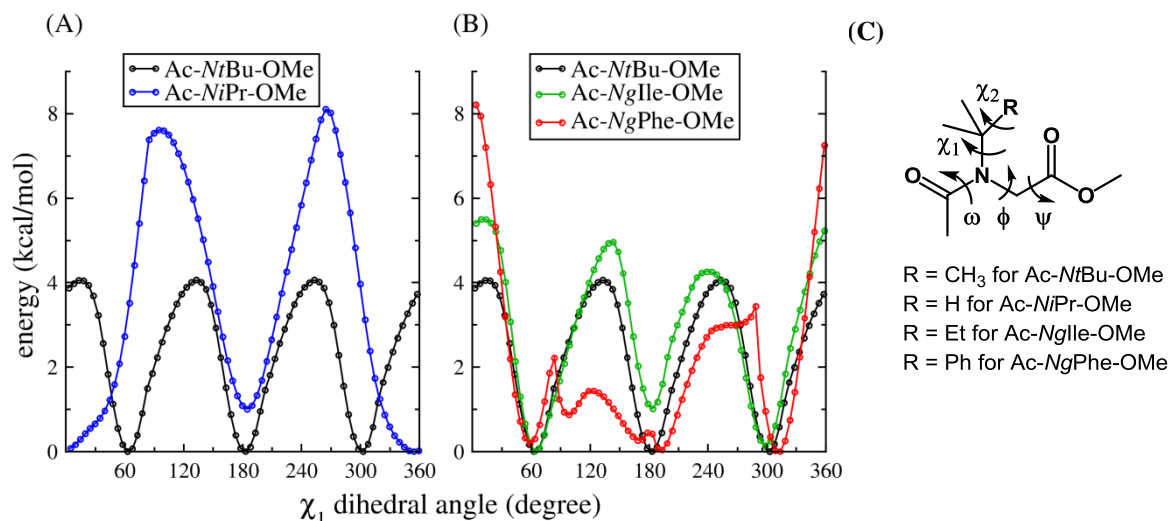


FIGURE 5 Energy diagram of the total scan of the χ_1 dihedral angles of model peptoid monomers: (A) Models carrying the *tert*-butyl side chain (R=Me) in black and the isopropyl side chain (R=H) in blue; (B) Models carrying the *tert*-butyl side chain (R=Me) in black, the $NC\alpha$ -*gem*-dimethyl propyl side chain (R=Et) in green and the $NC\alpha$ -*gem*-dimethyl benzyl side chain (R=Ph) in red; (C) Chemical structure of the models and definition of the dihedral angles : ω [C _{α} (i-1); C(i-1); N; C _{α}], ϕ [C(i-1); N; C _{α} ; C], ψ [N; C _{α} ; C; O], χ_1 [C(i-1); N; NC _{α} ; NC _{β} R] or [C(i-1); N; NC _{α} ; H] for the Ac-*Ni*Pr-OMe model

As recently reported, the side chain χ_1 dihedral angle of *Nt*Bu peptoid units differs significantly from that of peptoid monomers bearing a disubstituted side chain such as at the $NC\alpha$ carbon as for example an isopropyl side chain.¹⁹ For the Ac-*Nt*Bu-OMe model, three minima of equal energies were observed on the energy diagram for χ_1 values around $+60^\circ$, $\pm 180^\circ$ and -60° (300°) (Figure 5A). These staggered conformations prevent steric clashes between the Me groups and the amide carbonyl group of residue (i-1). By contrast, for the Ac-*Ni*Pr-OMe model, two minima were observed for χ_1 values around 0° and $\pm 180^\circ$. The lowest energy minimum corresponds to the eclipsed conformation with the $NC\alpha$ -H bond facing the C=O bond. For the Ac-*Ng*Ile-OMe model, three minima were observed corresponding to those observed for the Ac-*Nt*Bu-OMe model. The two lowest energy minima correspond to gauche conformations ($+60^\circ$ and -60° (300°)) and the third minimum corresponds to the anti-conformation (180°) (Figure 5B). The anti-conformation is 1 kcal/mol higher in energy than the gauche conformation due to a small steric clash between the ethyl CH₃ group and the backbone C _{α} protons. For the Ac-*Ng*Phe-OMe model, three minima centered at about $+60^\circ$, $\pm 180^\circ$ and -60° (300°) were also observed, but the profile of the energy diagram between these minima is unique. In this case, the χ_2 dihedral angle corresponding to the phenyl group rotation is also an important factor. However, the three lowest energy minima correspond to those observed for the Ac-*Nt*Bu-OMe model.

Peptoid oligomers with *cis*-amide bonds adopt a structure similar to the polyproline type I helix and the helical screw sense is induced by the stereochemistry of α -chiral side chains. Recently, we reported that achiral *Nt*Bu-based peptoids may also adopt a PPI-like structure stabilized by weak backbone CH \cdots O=C interactions and side chain *t*Bu \cdots *t*Bu London interactions.¹⁹ The same should be

observed in peptoid oligomers comprised of *N*C α -*gem*-dimethylated units. We have therefore performed a 40 ns molecular dynamic (MD) simulation of peptoid hexamer **18**. The initial structure was generated with backbone dihedral angles (ω, Φ, Ψ)=($0^\circ, -90^\circ, \pm 180^\circ$) near the polyproline type I helix and the side chain χ_1 dihedral angles were chosen according to the energy minima observed during the scan of the χ_1 dihedral angle. The χ_1 values were therefore initially fixed at $+60^\circ$ for the *N*tBu units, at $\pm 180^\circ$ for the *N*gPhe units and at -60° for the *N*gIle units. In the course of the MD simulation, the helical conformation was maintained revealing the stability of this structuration that closely resembles the PPI helix (Figure 6 and Supporting Information Figure S3).

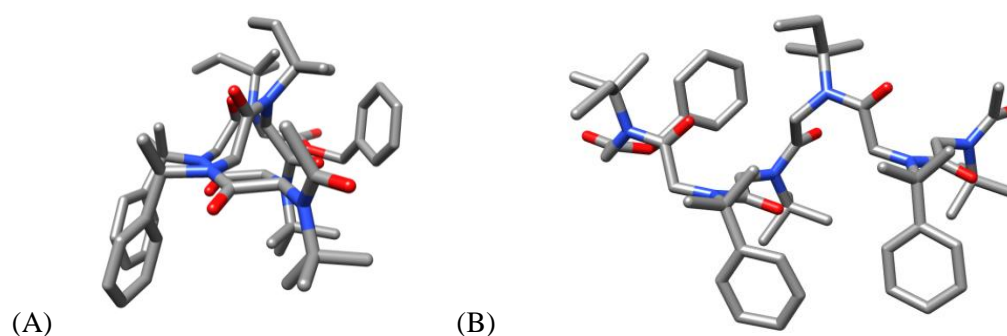


FIGURE 6 Model of hexamer **18** obtained by molecular dynamic (A) view perpendicular to the helical axis and (B) view parallel to the helical axis

Monitoring of the χ_1 dihedral angle variation over the course of the simulation as expected showed that rotation of the *tert*-butyl group occurred with three privileged positions ($\chi_1 = +60^\circ, -60^\circ$ or 180°) (Supporting Information Figure S2). By contrast, in the case of the *N*C α -*gem*-dimethylated side chains no rotation was observed during the simulation, apart from in the very beginning. Indeed, the χ_1 dihedral angle for the *N*gPhe units rapidly reached approximately -60° , which is identical to those of the *N*gIle units. This χ_1 dihedral angle of -60° corresponds to a spatial arrangement where the R substituents of the *N*C α -*gem*-dimethylated side chains are pointing away from the helical axis. According to this model, the formation of a PPI-like helical structure with outward distribution of the R groups is thus favored for peptoid oligomers incorporating *N*C α -*gem*-dimethylated side chains.

4 CONCLUSION

We have shown the high *cis*-directing effect of *N*C α -*gem*-dimethylated side chains by NMR spectroscopy studies of monomeric and trimeric peptoid models. Hexamers carrying *N*C α -*gem*-dimethylated side chains were furthermore obtained in solution by the submonomer method or a convergent fragment-coupling approach. The privileged positioning of the R group of the *N*C α -*gem*-dimethylated side chains was scrutinized according to the χ_1 torsion angle value by determining the total energy of peptoid models with the acetamide in the *cis* conformation. As observed for the *tert*-butyl side chain, staggered conformations preventing steric clashes between the methyl groups and the amide carbonyl group of residue (i-1) were preferred. A model of the PPI-type helix was constructed and studied by molecular dynamics simulations. This helical conformation appeared to be highly favorable although the achiral side chains do not allow controlling the helix direction *i.e.* the sign of Φ dihedral angle ($\approx -90^\circ$ or $+90^\circ$).¹⁹ Indeed in peptoid folding, the chirality of the side chains is critical to get well-folded secondary structures of defined handedness. This aspect has to be taken into account in the future design of *N*C α -*gem*-dimethylated *N*-substituted glycine oligomers mimicking specific peptide sequences.

Overall, these novel *NC α -gem*-dimethylated side chains represent a valuable addition to the “toolbox” for the construction of folded functionalized peptoid oligomers. This family of side chains retains structural diversity while maintaining a high degree of conformational control. The close mimic of peptide sequence is a crucial subject in a drug discovery context and these novel side chains will, for example, enable careful structure-activity relationship studies in the domain of peptoid-protein recognition.

ACKNOWLEDGMENT

We gratefully thank the French Ministry of Higher Education and Research for the grant to RS. We are grateful to M. Lereboure for mass spectrometry analysis (UCA PARTNER). Computations have been performed on the supercomputer facilities of the Mésocentre Clermont Auvergne. This work was supported by the ANR project ARCHIPEP.

¹R. N. Zuckermann, J. M. Kerr, S. B. H. Kent, W. H. Moos, *J. Am. Chem. Soc.* **1992**, *114*, 10646.

²A. S. Culf, R. J. Ouellette, *Molecules* **2010**, *15*, 5282.

³R. N. Zuckermann, T. Kodadek, *Curr. Opin. Mol. Ther.* **2009**, *11*, 299.

⁴C. W. Wu, K. Kirshenbaum, T. J. Sanborn, J. A. Patch, K. Huang, K. A. Dill, R. N. Zuckermann, A. E. Barron, *J. Am. Chem. Soc.* **2003**, *125*, 13525.

⁵N. H. Shah, G. L. Butterfoss, K. Nguyen, B. Yoo, R. Bonneau, D. L. Rabenstein, K. Kirshenbaum, *J. Am. Chem. Soc.* **2008**, *130*, 16622.

⁶B. C. Gorske, E. M. Mumford, C. G. Gerrity, I. Ko, *J. Am. Chem. Soc.* **2017**, *139*, 8070.

⁷J. A. Crapster, I. A. Guzei, H. E. Blackwell, *Angew. Chem. Int. Ed.* **2013**, *52*, 5079.

⁸K. Huang, C. W. Wu, T. J. Sanborn, J. A. Patch, K. Kirshenbaum, R. N. Zuckermann, A. E. Barron, I. Radhakrishnan, *J. Am. Chem. Soc.* **2006**, *128*, 1733.

⁹R. V. Mannige, T. K. Haxton, C. Proulx, E. J. Robertson, A. Battigelli, G. L. Butterfoss, R. N. Zuckermann, S. Whitelam, *Nature* **2015**, *526*, 415.

¹⁰R. Gopalakrishnan, A. I. Frolov, L. Knerr, W. J. Drury III, E. Valeur, *J. Med. Chem.* **2016**, *59*, 9599.

¹¹B. C. Gorske, J. R. Stringer, B. L. Bastian, S. A. Fowler, H. E. Blackwell, *J. Am. Chem. Soc.* **2009**, *131*, 16555.

¹²C. Caumes, O. Roy, S. Faure, C. Taillefumier, *J. Am. Chem. Soc.* **2012**, *134*, 9553.

¹³O. Roy, G. Dumonteil, S. Faure, L. Jouffret, A. Kriznik, C. Taillefumier, *J. Am. Chem. Soc.* **2017**, *139*, 13533.

¹⁴O. Roy, C. Caumes, Y. Esvan, C. Didierjean, S. Faure, C. Taillefumier, *Org. Lett.* **2013**, *15*, 2246.

¹⁵D. Gimenez, J. A. Aguilar, E. H. C. Bromley, S. L. Cobb, *Angew. Chem. Int. Ed.* **2018**, *57*, 10549.

¹⁶J. Seo, A. E. Barron, R. N. Zuckermann, *Org. Lett.* **2010**, *12*, 492.

¹⁷R. Shyam, N. Charbonnel, A. Job, C. Blavignac, C. Forestier, C. Taillefumier, S. Faure, *ChemMedChem* **2018**, *13*, 1513.

¹⁸G. Dumonteil, N. Bhattacharjee, G. Angelici, O. Roy, S. Faure, L. Jouffret, F. Jolibois, L. Perrin, C. Taillefumier, *J. Org. Chem.* **2018**, *83*, 6382.

¹⁹G. Angelici, N. Bhattacharjee, O. Roy, S. Faure, C. Didierjean, L. Jouffret, F. Jolibois, L. Perrin, C. Taillefumier, *Chem. Commun.* **2016**, *52*, 4573.

²⁰T. T. Talele, *J. Med. Chem.* **2018**, *61*, 2166.

²¹C. Toniolo, M. Crisma, F. Formaggio, C. Peggion, *J. Pept. Sci.* **2001**, *60*, 396.

²²Gaussian 09, Revision D.01, M. J. Frisch, G. W. Trucks, H. B. Schlegel, G. E. Scuseria, M. A. Robb, J. R. Cheeseman, G. Scalmani, V. Barone, G. A. Petersson, H. Nakatsuji, X. Li, M. Caricato, A. Marenich, J. Bloino, B. G. Janesko, R. Gomperts, B. Mennucci, H. P. Hratchian, J. V. Ortiz, A. F. Izmaylov, J. L. Sonnenberg, D. Williams-Young, F. Ding, F. Lipparini, F. Egidi, J. Goings, B. Peng, A. Petrone, T. Henderson, D. Ranasinghe, V. G. Zakrzewski, J. Gao, N. Rega, G. Zheng, W. Liang, M. Hada, M. Ehara, K. Toyota, R. Fukuda, J. Hasegawa, M. Ishida, T. Nakajima, Y. Honda, O. Kitao, H. Nakai, T. Vreven, K. Throssell, J. A. Montgomery, Jr., J. E. Peralta, F. Ogliaro, M. Bearpark, J. J. Heyd, E. Brothers, K. N. Kudin, V. N. Staroverov, T. Keith, R. Kobayashi, J. Normand, K. Raghavachari, A. Rendell, J. C. Burant, S. S. Iyengar, J. Tomasi, M. Cossi, J. M. Millam, M. Klene, C. Adamo, R. Cammi, J. W. Ochterski, R. L. Martin, K. Morokuma, O. Farkas, J. B. Foresman, and D. J. Fox, Gaussian, Inc., Wallingford CT, 2016.

²³E. F. Pettersen, T. D. Goddard, C. C. Huang, G. S. Couch, D. M. Greenblatt, E. C. Meng, T. E. Ferrin, *J. Comput. Chem.* **2004**, *25*, 1605.

-
- ²⁴ J.C. Phillips, R. Braun, W. Wang, J. Gumbart, E. Tajkhorshid, E. Villa, C. Chipot, R. D. Skeel, L. Kale, K. Schulten, *J. Comput. Chem.* **2005**, *26*, 1781.
- ²⁵ A.D. MacKerell, M. Feig, C.L. Brooks III, *J. Comput. Chem.* **2004**, *25*, 1400.
- ²⁶ W. Humphrey, A. Dalke, K. Schulten, *J. Mol. Graphics* **1996**, *14*, 33.
- ²⁷ C. Caumes, T. Hjelmgaard, R. Remuson, S. Faure, C. Taillefumier, *Synthesis* **2011**, *2*, 257.
- ²⁸ H. Aliouat, C. Caumes, O. Roy, M. Zouikri, C. Taillefumier, S. Faure, *J. Org. Chem.* **2017**, *82*, 2386.